

Excited fermions on kinks and the Dirac sea

Danial Saadatmand^{1,2} and Herbert Weigel¹

¹*Institute for Theoretical Physics, Physics Department, Stellenbosch University,
Matieland 7602, South Africa*

²*National Institute for Theoretical and Computational Sciences (NITheCS), Stellenbosch University Node,
Matieland 7602, South Africa*



(Received 7 December 2022; accepted 18 January 2023; published 8 February 2023)

We study quantum effects of recently discovered kink solitons which are constructed self-consistently by coupling to a single, excited fermion bound state. Our studies are based on the observation that in a semiclassical expansion the energies of this single level and of the Dirac sea should be treated equally. For these kink solutions we compute the energy of the Dirac sea as the fermion vacuum polarization energy. We find it to be substantial and to typically outweigh the energy gain from binding the single level.

DOI: [10.1103/PhysRevD.107.036006](https://doi.org/10.1103/PhysRevD.107.036006)

I. INTRODUCTION AND MOTIVATION

By Derrick's theorem [1] scalar field theories in one time and one space dimension ($D = 1 + 1$) wherein spontaneous symmetry breaking produces discrete degenerate vacua, are almost certain to contain (static) soliton solutions. These solutions have localized energy densities [2–4]. Low-dimensional soliton models are frequently considered as toy models for more complex theories in higher dimensions that have applications in many branches of physics: in cosmology [5], condensed matter physics [6,7], as well as hadron [8] and nuclear physics [9].

The field equation for a soliton is equivalent to minimizing its classical energy, E_{cl} . The leading, one-loop quantum correction to E_{cl} is the renormalized sum of the shifts of the zero-point energies of the quantum fluctuations. These shifts reflect the polarization of the vacuum induced by the soliton and thus this quantum correction is frequently called the vacuum polarization energy E_{VPE} (VPE). By now techniques have been developed that make it relatively straightforward to compute the VPE in $D = 1 + 1$ [10,11]; this is particularly the case when the potential for the quantum fluctuations is reflection symmetric. In general, E_{cl} and E_{VPE} exhibit different dependences on the model parameters. This feature is, for example, fundamental for the soliton picture of baryons in effective theories for quantum chromodynamics [12]. If the model parameters are chosen such that $E_{\text{cl}} \approx E_{\text{VPE}}$ one would expect that

higher-loop corrections are not negligible.¹ In such cases the VPE is not a reliable approximation for the quantum correction and its computation is merely of academic interest. Of course, this observation does not at all lessen the value of the groundbreaking studies on the VPE about half a century ago [14].

Yet, there are scenarios in which the VPE is indeed of significant importance and must be included. First, E_{cl} may be degenerate with respect to a certain (variational) parameter for the soliton but E_{VPE} is not.² In that case the VPE is decisive for the favorable soliton configuration albeit $E_{\text{cl}} \gg E_{\text{VPE}}$. Ref. [11] explores cases in which the inclusion of the VPE even destabilizes classically stable solitons (Higher-loop corrections may reverse this picture.). Second, the field equations are usually derived by minimizing an energy functional. This functional may contain components that in some expansion scheme are of the same order as the VPE. This feature can be delicate because the particular parameter dependences may be hidden when the model is constructed in terms of dimensionless variables and coordinates. It is this scenario that we focus on in this study. Third, with different topological sectors and associated topological charges Q , the VPE may be decisive for binding energies as in $E(2Q) - 2E(Q)$ [15].

The second scenario described above applies to models that recently attracted renewed interest. In these models a scalar boson with a nonlinear self-interaction that allows spontaneous symmetry breaking has a Yukawa coupling with a fermion. Typically the scalar field assumes a kink type structure connecting different vacua at positive and negative

Published by the American Physical Society under the terms of the [Creative Commons Attribution 4.0 International license](https://creativecommons.org/licenses/by/4.0/). Further distribution of this work must maintain attribution to the author(s) and the published article's title, journal citation, and DOI. Funded by SCOAP³.

¹See e.g. Ref. [13] for estimates beyond one loop.

²Translational invariance usually holds for both, though there are exceptions [10].

spatial infinity (and is thus topologically stable). Novel local minima of the energy functional were obtained [16–18] when the scalar couples to a single fermion that dwells in an excited bound state. We call these configurations local minima because the fermion could decay into a lower energy state while the kink radiates small amplitude fluctuations without changing its topological structure. The resulting configuration would have a smaller total energy and the classical kink mass would be its lower bound. We want to revisit these local minima for two reasons. First, in their construction the Dirac sea contribution was omitted. As we will explain later, in any suitable expansion scheme this contribution to the energy is of the same order as the one from the single level. Second, solutions with the single fermion occupying a negative energy level were also constructed. The Dirac sea must be included to give a physical interpretation because the negative energy level is a hole in the sea. But then the solution to the field equation becomes the charge conjugation of a configuration where the boson couples to a positive energy fermion level.

The paper is organized as follows. In Sec. II we will give a formal and brief discussion on the role of the Dirac sea when a single fermion level is occupied. We will then review the construction procedure of Ref. [16] modified such that the hole character of the negative energy levels is respected. In Sec. IV we will list and explain the formulas relevant to compute the vacuum polarization energy in the no-tadpole renormalization scheme. We present the results of our numerical simulations in Sec. V and conclude with a summary in Sec. VI.

II. DIRAC SEA

In order to make the arguments from the introduction explicit, we start with a short discussion of the role of the Dirac sea when certain fermion levels with energy eigenvalues E_ν are occupied. For a charge conjugation invariant background we can formally, i.e. before regularization and renormalization, write the total energy as

$$E_{\text{tot}} = E_{\text{cl}} + \sum_{\nu} \eta_{\nu} |E_{\nu}| - \sum_{\nu} [\theta(-E_{\nu}) |E_{\nu}| - \theta(-E_{\nu}^{(0)}) |E_{\nu}^{(0)}|]. \quad (1)$$

Here E_{cl} is the classical energy of the scalar background and $\eta_{\nu} = 0, 1$ are occupation numbers that describe the occupation of particular levels. The second sum adds the Dirac sea contribution³ where we have subtracted the trivial background equivalent (indicated by the superscript). The difference in that second sum measures the change in the spectrum and is called the vacuum polarization energy (VPE).

³If the background was not charge conjugation variant we would write $\frac{1}{2} \sum_{\nu} |E_{\nu}|$ for the Dirac sea contribution. Even though the trace of the Dirac Hamiltonian vanishes formally, the two prescriptions may yield different results because particular regularization prescriptions may cause this trace to be no longer zero.

Typically only a single level is selected, call it n so that $\eta_n = 1$ and $\eta_{\nu \neq n} = 0$. We classify a configuration as *classically stable* if $E_{\text{cl}} + |E_n| \leq m$, where m is the mass of the Dirac field. The *kink* is the soliton for a model without fermions. Its classical energy is E_{kink} . We call a configuration whose total energy is $E_{\text{tot}} \leq m + E_{\text{kink}}$ *topologically stable* because the sum on the right-hand side is the minimal energy of the system of an isolated free fermion and a boson field with a nontrivial topological structure. This is a sensible comparison because the change required for the boson field to get from E_{cl} to E_{kink} does not alter that structure.

When $E_n > 0$ we simply occupy that level. It is more interesting to consider $E_n < 0$. Then we can write

$$\begin{aligned} |E_n| &= \sum_{\nu} [\theta(-E_{\nu}) |E_{\nu}| - \theta(-E_{\nu}^{(0)}) |E_{\nu}^{(0)}|] \\ &= - \sum_{\nu \neq n} \theta(-E_{\nu}) |E_{\nu}| + \sum_{\nu} \theta(-E_{\nu}^{(0)}) |E_{\nu}^{(0)}|, \end{aligned}$$

which means that we have created a hole in the Dirac sea corresponding to an antiparticle state. Obviously the inclusion of the Dirac sea is essential for a consistent particle or antiparticle interpretation of the solutions to the Dirac equation. The need for combining the level and sea contributions was actually noted quite early in the context of nontopological soliton models for baryons [19,20], though those studies only focused on the case when the lowest non-negative energy bound state was occupied. Also renormalization is an issue for those higher-dimensional models.

In our analysis we first follow the procedure of Ref. [16] and minimize $E_{\text{cl}} + |E_n|$ to construct the static kink profile Φ_n . We will subsequently compute the Dirac sea contribution for this kink profile. In principle the Dirac sea component must also be included when constructing the profile from the minimum condition for the total energy. However, that is quite complicated as highly nonlocal field equations (would) emerge. So far this has only been performed in variational approximations or in nonrenormalizable theories, cf. Refs. [21,22] for reviews.

III. THE KINK MODEL

In $D = 1 + 1$ the scalar field Φ is dimensionless while the fermion spinors Ψ have canonical energy dimension $\frac{1}{2}$. To make the Yukawa coupling constant g dimensionless we write the Lagrangian as⁴

$$\mathcal{L}_F = \frac{i}{2} [\bar{\Psi}, \not{\partial} \Psi] - \frac{g}{2} \sqrt{\lambda} \Phi [\bar{\Psi}, \Psi]$$

⁴For quantized fermion fields we should actually write the fermion part of the Lagrangian as

to properly account for charge conjugation. This gives rise to the factor $\text{sign}(E_n)$ in Eq. (3). The commutators are for the fermion creation and annihilation operators.

$$\mathcal{L} = \frac{1}{2} \partial_\mu \Phi \partial^\mu \Phi - \frac{\lambda}{4} \left(\Phi^2 - \frac{M^2}{2\lambda} \right)^2 + i \bar{\Psi} \not{\partial} \Psi - g \sqrt{\frac{\lambda}{2}} \bar{\Psi} \Phi \Psi. \quad (2)$$

Observe that λ has dimension energy squared and that $m = \frac{gM}{2}$ is the fermion mass from spontaneous symmetry breaking that generates the vacuum expectation value $\langle \Phi \rangle = \frac{\pm M}{\sqrt{2\lambda}}$. The field equations for the scenario in which the scalar field only couples to the level n are (with the convention $\gamma^0 = \sigma_1$ and $\gamma^1 = i\sigma_3$)

$$\begin{aligned} \partial_x^2 \Phi_n &= \lambda \Phi \left(\Phi_n^2 - \frac{M^2}{2\lambda} \right) + g \sqrt{\frac{\lambda}{2}} \text{sign}(E_n) \Psi_n^\dagger \sigma_1 \Psi_n \\ E_n \Psi_n &= -i\sigma_2 \partial_x \Psi_n + g \sqrt{\frac{\lambda}{2}} \Phi_n \sigma_1 \Psi_n. \end{aligned} \quad (3)$$

These equations are supplemented by the normalization condition $\int dx \Psi_n^\dagger \Psi_n = 1$. Accounting for the fermion source term in the scalar field equation has been phrased *backreaction* in Ref. [16].

In order to find the most generic, i.e. parameter independent, formulation and also for numerical practicality it is appropriate to introduce dimensionless quantities

$$\begin{aligned} \Phi_n(x) &= \frac{M}{\sqrt{2\lambda}} \phi(\xi) \quad \text{and} \quad \Psi_n(x) = \sqrt{\frac{M}{2}} \psi(\xi), \\ \text{where } \xi &= \frac{M}{2} x. \end{aligned} \quad (4)$$

For simplicity we omit the subscript on the new fields. After this transformation the normalization condition is $\int d\xi \psi^\dagger(\xi) \psi(\xi) = 1$. The field equations become

$$\begin{aligned} \phi''(\xi) &= 2\phi(\xi)(\phi^2(\xi) - 1) + g \frac{2\lambda}{M^2} \text{sign}(\epsilon) \psi^\dagger(\xi) \sigma_1 \psi(\xi) \\ \text{and } \epsilon \psi(\xi) &= -i\sigma_2 \psi'(\xi) + g\phi(\xi) \sigma_1 \psi(\xi), \end{aligned} \quad (5)$$

where $\epsilon = \frac{2E_n}{M}$ is also dimensionless and primes denote derivatives with respect to ξ . The dimensionless fermion mass in this parametrization is $m \sim g$.

The classical mass is the integral

$$\begin{aligned} E_{\text{cl}} &= \int dx \left[\frac{1}{2} (\partial_x \Phi(x))^2 + \frac{\lambda}{4} \left(\Phi^2(x) - \frac{M^2}{2\lambda} \right)^2 \right] \\ &= \frac{M^3}{8\lambda} \int d\xi [\phi'^2(\xi) + (\phi^2(\xi) - 1)^2] = \frac{M^3}{\lambda} \frac{\epsilon_{\text{cl}}}{4}, \end{aligned} \quad (6)$$

where we understand the last equation as the definition of ϵ_{cl} . Then we combine

$$E_{\text{cl}} + |E_n| = \frac{M^3}{4\lambda} \left[\epsilon_{\text{cl}} + \frac{2\lambda}{M^2} |\epsilon| \right]. \quad (7)$$

As in Ref. [19] we call this the *quasiclassical energy*. We make the important observation that the contribution from the fermion levels scales with the relative factor $\frac{2\lambda}{M^2}$. This, of course, is then also the case for the energy from the Dirac sea because that is the sum of the single fermion energies obtained from the very same wave equation. This different parameter dependence is not surprising since in a semiclassical expansion the VPE has an extra factor of \hbar . Apart from the above particle-hole interpretation we have thus another strong motivation to include the Dirac sea. In Ref. [16] only the particular parameter choice $M = \sqrt{2\lambda}$ was considered. To some extent this hides the crucial detail that the classic scalar and fermion quantum energies have different scaling behaviors.

Introducing upper and lower spinor components $\psi = \begin{pmatrix} u \\ v \end{pmatrix}$, the profiles are subject to the differential equations

$$\begin{aligned} \phi'' &= 2\phi(\phi^2 - 1) + \frac{4g\lambda}{M^2} \text{sign}(\epsilon) uv, \\ u' &= \epsilon v - g\phi u \quad \text{and} \quad v' = -\epsilon u + g\phi v. \end{aligned} \quad (8)$$

For $g = 0$ the soliton is the well-known *kink*, $\phi(x) = \tanh(x)$. For completeness we recall that one then finds $\epsilon_{\text{cl}} = \frac{4}{3}$, or $E_{\text{cl}} = E_{\text{kink}} = \frac{M^3}{3\lambda}$. The kink is odd under spatial reflection. This reflection property is maintained when g is smoothly increased and we can write

$$\epsilon_{\text{cl}} = \int_0^\infty d\xi [\phi'^2(\xi) + (\phi^2(\xi) - 1)^2]. \quad (9)$$

From $\phi(-\xi) = -\phi(\xi)$ it is furthermore obvious that there are two parity cases for the fermion spinors. The first has even u and odd v ; the second has even v and odd u . These cases are called *A*- and *B*-type solutions in Ref. [16]. We keep that notation. Additional integer labels on *A* and *B* count the number of zero crossings of u on the half line $x \geq 0$, including the one at $x = 0$ for the *B*-type.

Equations (8) are invariant when changing the signs of u and ϵ but keeping the sign of v . Hence the spectrum is symmetric for a given profile ϕ . Furthermore, occupying a particle or an antiparticle level with equal $|\epsilon|$ (which is equivalent to digging a hole into the Dirac sea) yield equivalent solutions.

The fermion equations have two $\epsilon = 0$ solutions

$$\begin{aligned} u(\xi) &= N \exp \left[-g \int^\xi d\xi' \phi(\xi') \right], \quad v(\xi) = 0 \quad \text{and} \\ u(\xi) &= 0, \quad v(\xi) = N \exp \left[g \int^\xi d\xi' \phi(\xi') \right]. \end{aligned} \quad (10)$$

Without loss of generality we take $\text{sign}(\phi) = \text{sign}(\xi)$. Then only the first solution is normalizable so that there is

exactly one normalizable zero mode in the A_0 channel for any prescribed ϕ . In either case $uv = 0$ so that there is no fermionic source term in the wave equation for ϕ which is then solved by the kink profile.

IV. FERMION VPE

The construction of fermion continuum scattering solutions with a kink type background is not straightforward because the mass parameters at positive and negative spatial infinity have opposite signs; though this is only a problem for practical calculations rather than a conceptual one. Fortunately for a static system which is invariant under charge conjugation we can formally write the effective action, from which the VPE is extracted, as

$$\int \frac{d\omega}{2\pi} \text{TrLog}[\omega - H] = \frac{1}{2} \int \frac{d\omega}{2\pi} \text{TrLog}[\omega^2 - H^2], \quad (11)$$

where the trace goes over the eigenstates of the Dirac Hamiltonian H . This shows that the VPE of the fermion system can be obtained from the average VPE of two scalar systems [23]. More explicitly we have from Eq. (8)

$$H = \begin{pmatrix} 0 & -\partial_\xi + g\phi \\ \partial_\xi + g\phi & 0 \end{pmatrix} \quad \text{so that} \\ H^2 = \begin{pmatrix} -\partial_\xi^2 - g\phi' + g^2\phi^2 & 0 \\ 0 & -\partial_\xi^2 + g\phi' + g^2\phi^2 \end{pmatrix}. \quad (12)$$

The potentials of the two scalar systems are straightforwardly identified as

$$V_S = g^2(\phi^2 - 1) - g\phi' \quad \text{and} \quad \widetilde{V}_S = g^2(\phi^2 - 1) + g\phi'. \quad (13)$$

With ϕ being odd, these potentials are even in the coordinate ξ and the VPE in the no-tadpole renormalization scheme can be computed by standard techniques [11,21]. In this scheme, the Lagrangian counterterm proportional to $(\Phi^2 - \langle \Phi \rangle^2)$ is adjusted such that there are no quantum corrections to the vacuum expectation value of the scalar field. The related, ultraviolet-divergent tadpole Feynman

diagram is a loop with a single insertion of the potential and thus does not depend on the Fourier momentum of V_S (or \widetilde{V}_S). In turn the diagram is completely canceled by this counterterm.

The basic ingredients for the nonperturbative part of the VPE are the Jost functions for imaginary momenta in the positive and negative parity channels. The Jost functions are extracted from the Jost solutions $f(k, \xi)$ which are solutions to the Schroedinger equations with the potentials V_S and \widetilde{V}_S . Asymptotically ($\xi \rightarrow \infty$) the Jost solutions are incoming plane waves. In general there are contributions to the VPE from the bound and continuum scattering states. The latter contribution is the momentum integral over the single particle energies weighted by the density of states. In a given parity channel the difference of the densities of states with and without the background potential is the derivative of the phase shift with respect to the momentum [24]. Next we use that the phase shift is the logarithm of the Jost function which has simple zeros at the imaginary momenta of the bound state energies. Hence, when writing that continuum integral as a contour integral in the complex momentum plane the singularities and residues resulting from the logarithmic derivative cancel the explicit bound state contributions to the VPE. All what is left stems from the discontinuity of the dispersion relation $\omega = \sqrt{k^2 + g^2}$ along the imaginary axis.⁵ With $k = it$ we are then left with an integral over $t \in [g, \infty]$.

To facilitate the calculation we factorize the plane-wave component of the Jost solution after continuing to imaginary momenta: $f(it, \xi) = e^{-t\xi} G(t, \xi)$ and establish the second-order differential equation

$$G''(t, \xi) = 2tG'(t, \xi) + \sigma(\xi)G(t, \xi). \quad (14)$$

Here σ is either V_S or \widetilde{V}_S . With the boundary condition $\lim_{\xi \rightarrow \infty} G(t, \xi) = 1$ we extract the Jost functions from $G(t, 0)$ and $G'(t, 0) = \frac{\partial G(t, \xi)}{\partial \xi} \Big|_{\xi=0}$ to accommodate the reflections properties (of the scattering wave function) for the positive and negative parity channels. Putting things together yields the vacuum polarization energy [11,21]

$$\epsilon_{\text{VPE}}[\sigma] = \int_0^\infty \frac{d\tau}{2\pi} \left\{ \ln \left[G(t, 0) \left(G(t, 0) - \frac{1}{t} G'(t, 0) \right) \right] - \frac{\langle \sigma \rangle}{t} \right\}_{t=\sqrt{\tau^2 + g^2}}. \quad (15)$$

Here we have introduced the integration variable $\tau = \sqrt{t^2 - g^2}$ to mitigate an integrable singularity at $t = g$.

⁵The imaginary axis formalism also avoids ambiguities from the multivalued logarithm of complex numbers that might have occurred in earlier studies on the fermion VPE from (pseudo) scalar backgrounds [23,25,26].

The two factors under the logarithm are the Jost functions in the odd and even parity channels, respectively while the subtraction with $\langle \sigma \rangle = \int_0^\infty d\xi \sigma(\xi)$ takes out the contribution that is associated with the tadpole diagram. Since that diagram and the counterterm cancel exactly, the subtraction in Eq. (15) implements the no-tadpole renormalization condition and renders the τ integral ultraviolet finite.

The total renormalized VPE is simply the sum (note the overall sign for a fermion)

$$E_{\text{VPE}} = -\frac{M}{4}(\epsilon_{\text{VPE}}[V_S] + \epsilon_{\text{VPE}}[\tilde{V}_S]). \quad (16)$$

For this average the subtraction under the integral in Eq. (15) is proportional to

$$\frac{1}{2}\langle V_S + \tilde{V}_S \rangle = g^2 \int_0^\infty d\xi (\phi^2 - 1). \quad (17)$$

It indeed equals the contribution from the counterterm that cancels all quantum corrections to the scalar vacuum expectation value.

V. NUMERICAL RESULTS

The numerical treatment Eqs. (8) is simplified by the parity properties that we have discussed in Sec. III. For a given parity channel it suffices to solve the equations on the half line $\xi \geq 0$. In addition to $\phi(0) = 0$ we have the following initial conditions for the spinors

$$\begin{aligned} \text{A-type: } u(0) &= 1, & v(0) &= 0 \quad \text{and} \\ \text{B-type: } u(0) &= 0, & v(0) &= 1. \end{aligned} \quad (18)$$

At a large ξ_{max} in both channels the boundary conditions

$$u(\xi_{\text{max}}) = 1 \quad \text{and} \quad v(\xi_{\text{max}}) = \frac{g-t}{\epsilon} \quad \text{with} \quad t = \sqrt{g^2 - \epsilon^2} \quad (19)$$

ensure that the fermion profiles are proportional to $e^{-t\xi}$ outside the realm of $\phi(\xi)$ as required for a bound state with $|e| < g$.

To self-consistently construct the profile that minimizes the quasiclassical energy $\epsilon_{\text{cl}} + \frac{2\lambda}{M^2}|e|$ we first compute the bound state energies and wave functions as a function of g for the kink profile $\phi(x) = \tanh(x)$. In this process the fermion differential equations in Eq. (8) are solved with the initial and boundary conditions from Eqs. (18) and (19). Solutions that are continuous over the whole ξ half line only exist for particular values of ϵ . These are the energy eigenvalues which we identify with a nested interval algorithm. The resulting fermion profile functions are normalized to $\int_0^\infty d\xi [u^2 + v^2] = \frac{1}{2}$. At small g only the A_0 zero mode is bound. We then increase g until the desired mode gets bound with a significant binding energy. This desired mode could, for example, be B_1 which is the one with the lowest positive energy eigenvalue in the negative parity channel. We substitute the corresponding fermion profiles into the differential equation for ϕ . For this equation we employ a shooting method for the slopes of $\phi(\xi)$ at $\xi = 0$ and $\xi = \xi_{\text{max}} \gg 1/g$ such that both ϕ and ϕ' are continuous. We then iterate this procedure until convergence under the iteration is observed. This convergence

is measured by $\epsilon_{\text{cl}} + \frac{2\lambda}{M^2}|e|$ being stationary. As we further increase g , guessing a good initial profile ϕ becomes problematic as we observe that the success of the iteration is quite sensitive to this initial guess. In most cases a linear (over)relaxation procedure has proven to be successful: Assume $\phi^{(1)}$ and $\phi^{(2)}$ are self-consistent solutions for Yukawa couplings $g_1 \lesssim g_2$, respectively. Then

$$\phi^{(3)}(\xi) = \phi^{(1)}(\xi) + \zeta \frac{\phi^{(2)}(\xi) - \phi^{(1)}(\xi)}{g_2 - g_1} (g_3 - g_1), \quad (20)$$

with the fudge factor $\zeta \gtrsim 1$, turns out to be a good initial guess for the profile associated with $g_3 \gtrsim g_2$.

In all numerical simulations we set the scale by choosing $M = 2$ and eventually vary λ . Stated otherwise, to get energies in terms of physical units, the results below have to be multiplied by $M/2$ with M measured in electron volts, for example. This choice for M is convenient since then $E = \frac{2}{M}\epsilon = \epsilon$.

In Ref. [16] solutions to Eqs. (8) were obtained for many choices of the occupied level. To make our arguments clear it suffices to focus on the lowest lying excitations in the two parity channels B_1 and A_1 . For these channels we have reproduced the kink solitons of Ref. [16] when $M^2 = 2\lambda$. In addition we have constructed solutions deviating from this particular relation between the model parameters. A few profiles are displayed in Fig. 1. Their construction turned out to be somewhat cumbersome for $M^2 < 2\lambda$ since this effectively corresponds to increasing g in the differential equation for ϕ . Accordingly the larger the ratio $\frac{\lambda}{M^2}$, the larger the deviation of the kink profile from $\tanh(\xi)$.

For the discussion of the energetic stability we recall from the previous sections the three energies to consider: (i) classical E_{cl} , (ii) quasiclassical $E_{\text{cl}} + E$, and (iii) semiclassical $E_{\text{tot}} = E_{\text{cl}} + E + E_{\text{VPE}}$. As argued in Secs. III (i) and (iii) are leading and subleading fermion contributions, respectively, while (ii) cannot be associated with a particular truncation of an expansion scheme.

To investigate the (quasi)classical stability ($E + E_{\text{cl}} \leq g$) we consider the numerical results for Eq. (7) in Tables I, II and III. We stress that this is not absolute stability, as the fermion could still move to the ever present zero mode and the energy would be that of the classical kink, $E_{\text{kink}} = \frac{M^3}{3\lambda}$ plus the fermion VPE for the kink (to be discussed below). We observe this stability when the Yukawa coupling g exceeds a certain value. With $M^2 = 2\lambda$ this is at about $g = 3$ and $g = 4$ for the B_1 and A_1 channels, respectively. As we detune λ from this relation, these critical values decrease as λ increases and vice versa. This opposite behavior is essentially due to the λ dependence of E_{cl} . We recognize that E_{cl} is smaller for the A_1 channel than for the B_1 channel when $M^2 \leq 2\lambda$. This is remarkable because the distortion of the A_1 profile is larger in the sense that it is wider than its B_1 counterpart.

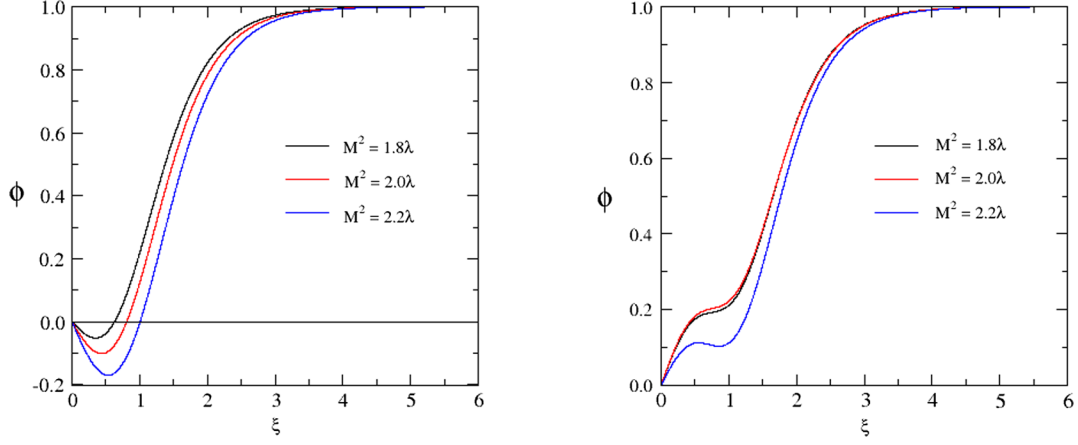


FIG. 1. Kink profiles in the B_1 (left panel) and A_1 (right panel) channels for $g = 4.0$ and deviations from $M^2 = 2\lambda$. The profile on the negative half line is obtained from the reflection $\phi(\xi) = -\phi(-\xi)$.

We next compute the VPE. Occupying the zero mode A_0 implies $uv = 0$, according to Eq. (10). Hence, there is no backreaction in this case and $\phi(\xi) = \tanh(\xi)$. For this scenario we find $E_{\text{VPE}} = 0.348, 0.607, 0.943$ and 1.359 for $g = 2.0, g = 3.0, g = 4.0$ and $g = 5.0$, respectively. The $g = 2.0$ result is analytically known to be $M(\frac{1}{\pi} - \frac{1}{4\sqrt{3}}) \approx 0.3479$ [23] favorably confirming our numerical simulation. The VPE results for the A_0 level do not depend on the particular value for λ since this parameter enters via the distortion of the scalar profile only when $uv \neq 0$ and as an overall factor in E_{cl} . The resulting total energies are listed in Table IV. In our approximation scheme these are the lowest energies for the kink topology. In this channel we have $E = 0$ and $E_{\text{VPE}} < g$ so that the configuration is topologically stable.

Finally, Tables V, VI and VII contain our numerical results for the fermion contribution to the energy for configurations that include the backreaction from a particular fermion level on the kink. This contribution has two components, the energy of the explicitly occupied level and the VPE from the Dirac sea. The latter is our main novel result. In all cases considered, the VPE adds positively and may indeed be substantial. Similar to the classical energy, the fermion VPE differs only slightly between the B_1 and A_1 channels. For small g the VPE for the A_1 channel is even less than for the B_1 channel. This suggests a lesser

polarization of the Dirac sea in the A_1 case. However, for both channels the fermion VPE is significantly larger than it is when occupying the A_0 mode. Hence, the backreaction has an important impact on the VPE.

In Table V we present the fermion energies in the B_1 and A_1 channels when $M^2 = 2\lambda$ but for different values of the Yukawa coupling g . For the B_1 channel we find the quasiclassical energy to obey $E + E_{\text{VPE}} < g$. This suggests that the fermionic piece could be stable by itself. However, that threshold is exceeded within the A_1 channel. In either case the gain in energy from binding the single level, $g - E$, is essentially compensated by the VPE. To discuss the topological (in)stability we must consider the semiclassical energy E_{tot} which includes the Dirac sea contribution. We find topological stability ($E_{\text{tot}} \leq g + E_{\text{kink}}$, with the $M^2 = 2\lambda$ values for $g + E_{\text{kink}}$ listed in Table I) merely for small g in the B_1 channel. For the A_1 channel it does not occur at all. The data in Tables VI and VII show that this picture does not change qualitatively when we vary λ (cf. Tables II and III, for the respective values of $g + E_{\text{kink}}$). For small g the level energy increases with the ratio $\frac{M^2}{\lambda}$ while the VPE decreases (in the considered λ range). As g increases this monotonic behavior disappears. The quasiclassical energy $E + E_{\text{VPE}}$ is still smaller than g in the B_1 channel for $g \leq 5$. This kinematic bound is always exceeded within the A_1 channel. Presumably this bound will also be exceeded for

TABLE I. Energies in Eq. (7) as functions of the Yukawa coupling g for the B_1 and A_1 channels with $M^2 = 2\lambda$. For $g = 0$ the classical mass is $E_{\text{kink}} = \frac{4}{3} \approx 1.333$.

g	B_1				A_1				
	E	E_{cl}	$E + E_{\text{cl}}$	$g + E_{\text{kink}}$	g	E	E_{cl}	$E + E_{\text{cl}}$	$g + E_{\text{kink}}$
2.6	1.433	1.670	3.103	3.933	2.8	2.227	1.536	3.764	4.133
3.0	1.370	1.812	3.183	4.333	3.0	2.140	1.721	3.861	4.333
4.0	1.039	2.231	3.270	5.333	4.0	2.069	2.079	4.148	5.333
5.0	0.715	2.540	3.255	6.333	5.0	1.749	2.542	4.292	6.333

TABLE II. Same as Table I for $M^2 = 1.8\lambda$ with $E_{\text{kink}} = \frac{3}{5} = 1.2$.

B_1					A_1				
g	E	E_{cl}	$E + E_{\text{cl}}$	$g + E_{\text{kink}}$	g	E	E_{cl}	$E + E_{\text{cl}}$	$g + E_{\text{kink}}$
2.6	1.346	1.584	2.930	3.8	3.0	2.090	1.595	3.685	4.2
3.0	1.227	1.765	2.992	4.2	3.5	2.036	1.799	3.835	4.7
3.5	1.026	2.006	3.032	4.7	4.0	1.875	2.068	3.944	5.2
4.0	0.812	2.223	3.035	5.2	4.5	1.716	2.286	4.003	5.7

TABLE III. Same as Table I for $M^2 = 2.2\lambda$ with $E_{\text{kink}} = \approx 1.467$.

B_1					A_1				
g	E	E_{cl}	$E + E_{\text{cl}}$	$g + E_{\text{kink}}$	g	E	E_{cl}	$E + E_{\text{cl}}$	$g + E_{\text{kink}}$
3.0	1.472	1.887	3.358	4.467	3.0	2.146	1.887	4.039	4.467
4.0	1.226	2.258	3.484	5.467	4.0	2.050	2.304	4.354	5.467
5.0	0.891	2.609	3.501	6.467	5.0	1.813	2.721	4.535	6.467

TABLE IV. Total energy for the A_0 channel for various model parameters.

M^2/λ	$E_{\text{kink}} + E_{\text{VPE}}$			
	$g = 2.0$	$g = 3.0$	$g = 4.0$	$g = 5.0$
1.8	1.548	1.807	2.143	2.559
2.0	1.681	1.940	2.276	2.692
2.2	1.815	2.074	2.410	2.826

TABLE V. The single-level fermion energies E and the renormalized Dirac sea contributions for the case $M^2 = 2\lambda$ as a function of the Yukawa coupling g . Here $E_{\text{tot}} = E + E_{\text{VPE}} + E_{\text{cl}}$. Left panel: B_1 channel, right panel: A_1 channel.

B_1					A_1				
g	E	E_{VPE}	$E + E_{\text{VPE}}$	E_{tot}	g	E	E_{VPE}	$E + E_{\text{VPE}}$	E_{tot}
2.6	1.433	0.714	2.147	3.817	2.8	2.227	0.693	2.920	4.456
3.0	1.370	0.990	2.360	4.172	3.0	2.140	0.945	3.091	4.812
4.0	1.039	2.031	3.079	5.310	4.0	2.069	1.999	4.068	6.147
5.0	0.715	3.439	4.154	6.694	5.0	1.749	3.687	5.436	7.978

TABLE VI. Same as Table V for $M^2 = 1.8\lambda$.

B_1					A_1				
g	E	E_{VPE}	$E + E_{\text{VPE}}$	E_{tot}	g	E	E_{VPE}	$E + E_{\text{VPE}}$	E_{tot}
2.6	1.346	0.755	2.101	3.685	3.0	2.090	0.984	3.074	4.639
3.0	1.227	1.066	2.293	4.058	3.5	2.036	1.492	3.528	5.327
3.5	1.026	1.597	2.623	4.629	4.0	1.875	2.245	4.120	6.188
4.0	0.812	2.237	3.049	5.272	4.5	1.716	2.990	4.706	6.992

TABLE VII. Same as Table V for $M^2 = 2.2\lambda$.

B_1					A_1				
g	E	E_{VPE}	$E + E_{\text{VPE}}$	E_{tot}	g	E	E_{VPE}	$E + E_{\text{VPE}}$	E_{tot}
3.0	1.472	0.933	2.405	4.292	3.0	2.146	0.942	3.088	4.975
4.0	1.226	1.871	3.097	5.355	4.0	2.050	2.014	4.064	6.368
5.0	0.891	3.236	4.127	6.736	5.0	1.813	3.612	5.425	8.146

TABLE VIII. The single-level fermion energies E and the renormalized Dirac sea contributions for the case $M^2 = 2\lambda$ as a function of the Yukawa coupling g . Left panel: B_{-1} channel, right panel: A_{-1} channel.

B_{-1}			A_{-1}		
g	E	E_{VPE}	g	E	E_{VPE}
3.0	-2.762	0.500	3.8	-3.419	0.841
4.0	-3.567	0.680	4.0	-3.592	0.892
5.0	-4.363	0.864	5.0	-4.481	1.133

large enough g in the B_1 channel because E cannot become less than zero.

In Ref. [16] also configurations that minimize

$$E_{\text{cl}} + \epsilon_n \quad \text{with} \quad \epsilon_n < 0$$

have been constructed. Even though such systems do not have a particle-hole interpretation, we have nevertheless computed the fermion VPE for B_{-1} and A_{-1} channels.⁶ These are the first available levels in the negative and positive parity channels. The resulting data are displayed in Table VIII. For these cases the binding of the level ($E + g$) is small, but so is the VPE and there is no absolute gain when compared to the mass of a free fermion.

VI. CONCLUSION

In this study we have computed the vacuum polarization energy (VPE) emerging from fermion fluctuations about recently observed solitons for scalar fields coupled to fermions in one time and one space dimension. These solutions deviate from the renowned kink by self-consistently accounting for the backreaction from a single fermion bound state level. We have argued that this VPE must be considered for two reasons, at least. First, it equals the contribution from the Dirac sea. This contribution is needed for a physically sensible picture when the selected level has a negative energy eigenvalue. Second, when the model parameters are consistently incorporated, the VPE is of the same order in a semiclassical expansion as the energy

eigenvalue of the single level. This was revealed by a careful analysis of the parameter dependence of the energy. Thereafter, fields and variables could be redefined to dimensionless quantities suitable for the numerical simulation.

We have found that the fermion VPE contribution is substantial and approximately outweighs the binding of the single level in the parameter regime that leads to a sizable backreaction. Nevertheless, that configuration may still be topologically stable for the case that the single fermion level is the first excited state and the Yukawa coupling is small; i.e. its total energy is less than that of a single free fermion and a kink without backreaction. For moderate and large couplings this stability is lost. In other channels it never occurs. We have not found a configuration that is absolutely stable as the total energy has always been larger than that of a free fermion combined with the translationally invariant scalar configuration. Stated otherwise, the local minima of the quasiclassical energy functional cease to exist for the semiclassical analog.

In a consistent quantum field theory calculation the Dirac sea contribution to the energy is obtained from the fermion effective action. Its nonlocal structure makes it impossible to construct the minimum of the semiclassical energy from a set of differential equations. Hence, a variational procedure [25] that minimizes this energy is the most suggestive extension of the current study.

In many considerations the boson VPE may be neglected compared to the fermion one because the latter scales with the number of internal degrees of freedom (for example, the number of colors in soliton models for the strong interaction). In the present model that number is unity and there is no (obvious) approximation scheme that favors the fermion VPE. We have seen that it strongly increases with the Yukawa coupling and for large enough coupling it dominates (presumably) and thus justifies the omission of the boson VPE. In any event, such a calculation would be even more cumbersome as a further backreaction must then be taken into account, that of the boson fluctuations on the fermion wave-functions. From the historic studies in Refs. [2,14] we expect the boson VPE to be negative and to some extent cancel the fermion counterpart that we computed here. These studies also suggest a not so obvious scenario in which the boson VPE is negligible against the fermion counterpart; the model without fermions also has

⁶The minus sign in the subscript is added for the negative energy eigenvalue [16].

the factor λ/M^2 for the boson VPE relative to the classical energy [21]. A consistent model in which higher-order boson quantum effects are small would thus require $M^2 \gg \lambda$. To nevertheless have a substantial backreaction from the fermion level a large Yukawa coupling will be needed. Exploring this parameter regime certainly is another interesting extension of the presented study.

In Ref. [16] scenarios with an additional explicit mass term $\mathcal{L}_m = -m_0 \bar{\Psi}\Psi$ were considered. With the kink connecting the two distinct vacua at $\langle \Phi \rangle = \pm \frac{M}{\sqrt{2}\lambda}$ at positive and negative spatial infinity, its inclusion would lead to different mass parameters, $m_0 \pm \frac{g}{2}M$, in the fermion sector. Such systems are destabilized by quantum effects [10,27].

The above discussions indicate that our estimate for the quantum corrections when kinks are bounded to excited

fermion levels leaves space for future extensions. Yet, it accounts for the important fact that contributions from distinct energy levels and the Dirac sea are of equal order in the semiclassical expansion. We have therefore combined these contributions and our estimate suggests that the Dirac sea contribution to the total energy outweighs the gain from binding single levels. This points towards an instability of such configurations.

ACKNOWLEDGMENTS

One of us (H.W.) thanks N. Graham for helpful discussions. H.W. is supported in part by the National Research Foundation of South Africa (NRF) by Grant No. 109497.

-
- [1] G. H. Derrick, *J. Math. Phys. (N.Y.)* **5**, 1252 (1964).
 - [2] R. Rajaraman, *Solitons and Instantons* (North Holland, Amsterdam, 1982).
 - [3] N. S. Manton and P. Sutcliffe, *Topological Solitons*, Cambridge Monographs on Mathematical Physics (Cambridge University Press, Cambridge, England, 2004).
 - [4] T. Vachaspati, *Kinks and Domain Walls: An Introduction to Classical and Quantum Solitons* (Cambridge University Press, Cambridge, England, 2010).
 - [5] A. Vilenkin and E. P. S. Shellard, *Cosmic Strings and Other Topological Defects* (Cambridge University Press, Cambridge, England, 2000).
 - [6] U. Schollwöck *et al.*, *Quantum Magnetism*, Lecture Notes in Physics (Springer, New York, 2004), Vol. 645.
 - [7] N. Nagaosa and Y. Tokura, *Nature Nanotech.* **8**, 899 (2013).
 - [8] H. Weigel, *Chiral Soliton Models for Baryons*, Lecture Notes in Physics (Springer, New York, 2008), Vol. 743.
 - [9] D. T. J. Feist, P. H. C. Lau, and N. S. Manton, *Phys. Rev. D* **87**, 085034 (2013).
 - [10] H. Weigel, *Phys. Lett. B* **766**, 65 (2017).
 - [11] N. Graham and H. Weigel, *Int. J. Mod. Phys. A* **37**, 2241004 (2022).
 - [12] E. Witten, *Nucl. Phys.* **B160**, 57 (1979).
 - [13] J. Evslin, *Phys. Lett. B* **822**, 136628 (2021).
 - [14] R. F. Dashen, B. Hasslacher, and A. Neveu, *Phys. Rev. D* **10**, 4114 (1974).
 - [15] N. Graham and H. Weigel, *Phys. Rev. D* **106**, 076013 (2022).
 - [16] V. Klimashonok, I. Perapechka, and Y. Shnir, *Phys. Rev. D* **100**, 105003 (2019).
 - [17] I. Perapechka and Y. Shnir, *Phys. Rev. D* **101**, 021701 (2020).
 - [18] V. A. Gani, A. Gorina, I. Perapechka, and Y. Shnir, *Eur. Phys. J. C* **82**, 757 (2022).
 - [19] R. Friedberg and T. D. Lee, *Phys. Rev. D* **15**, 1694 (1977).
 - [20] S. Kahana, G. Ripka, and V. Soni, *Nucl. Phys.* **A415**, 351 (1984).
 - [21] N. Graham, M. Quandt, and H. Weigel, *Spectral Methods in Quantum Field Theory* (Springer, New York, 2009), Vol. 777.
 - [22] R. Alkofer, H. Reinhardt, and H. Weigel, *Phys. Rep.* **265**, 139 (1996).
 - [23] N. Graham and R. L. Jaffe, *Nucl. Phys.* **B549**, 516 (1999).
 - [24] J. S. Faulkner, *J. Phys. C* **10**, 4661 (1977).
 - [25] E. Farhi, N. Graham, R. L. Jaffe, and H. Weigel, *Nucl. Phys.* **B585**, 443 (2000).
 - [26] S. S. Gousheh, A. Mohammadi, and L. Shahkarami, *Phys. Rev. D* **87**, 045017 (2013).
 - [27] T. Romańczukiewicz, *Phys. Lett. B* **773**, 295 (2017).